"Superlong" Metal–Metal Single Bonds in Bimetallic Complexes of Zirconium(III): Extended Hückel and ab Initio Self-Consistent Field/Configuration Interaction Study

Marie-Madeleine Rohmer and Marc Bénard*

Laboratoire de Chimie Quantique, ER 139 du CNRS, Institut Le Bel, Université Louis Pasteur, F 67000 Strasbourg, France

Received March 29, 1990

Quantum chemical calculations carried out on $[(C_5H_5)_2Zr(\mu\text{-}I)]_2$ (1), $[ZrCl_3(PH_3)_2]_2$ (2), and $[(C_5H_5)_2Zr(\mu\text{-}PH_2)]_2$ (3) indicate that the metal–metal bond length results from a compromise between the stabilization brought in by the metal–metal σ bond and the occurrence of repulsive H···H contacts. The extended Hückel analysis suggests and the ab initio self-consistent field/configuration interaction (SCF/CI) calculations carried out on 2 and 3 confirm that a substantial amount of through-space metal–metal coupling does exist at metal–metal distances larger than 3.5 Å characterized for 1 and related systems. Singlet–triplet (S–T) energy separations are computed at the CI level, using a basis of optimized natural orbitals. Computed S–T splittings are 8200 cm^{-1} for $[ZrCl_3(PH_3)_2]_2$ (2) (d_{Zr-Zr} = 3.169 Å) and 8500 cm^{-1} for $[(C_5H_5)_2Zr(\mu\text{-}PH_2)]_2$ (3) (d_{Zr-Zr} = 3.653 Å).

Introduction

A recent characterization of a series of dinuclear complexes of zirconium(III)[1-3] questions the reality of the metal–metal bond commonly postulated to explain the diamagnetism observed in these complexes. Some of the structurally characterized complexes of $(Zr_2)^{6+}$, like $Zr_2Cl_6(PEt_3)_4$ and related compounds, exhibit metal–metal distances ranging from 3.104 to 3.169 Å[4] and are assumed to be compatible with the existence of a single σ bond. The fulvalene derivative $(\eta^5{:}\eta^5\text{-}C_{10}H_8)[(\eta^5\text{-}C_5H_5)Zr(\mu\text{-}Cl)]_2$ displays a somewhat longer Zr–Zr distance of 3.233 Å,[5] but its diamagnetism is still interpreted in terms of a direct metal–metal bond. The problem arises from a series of Cp_2Zr^{III} dimers bridged by phosphido[1] or/and halide[1-3] ligands and characterized by metal–metal distances ranging from 3.524 Å in $(Cp_2Zr)_2(\mu\text{-}Cl)[\mu\text{-}P(CH_3)_2]$[1] to 3.669 Å in $[Cp_2ZrI]_2$.[2] These distances are considered too long to be compatible with a direct metal–metal bond, thus raising the question of the origin of the observed diamagnetism.[3] The purpose of the present work is to try to clear up these problems from a quantum chemical analysis carried out at both the extended Hückel and the ab initio SCF/CI levels.

Computational Details

Extended Hückel calculations[6] were carried out on $[Cp_2ZrI]_2$ (1) at various geometries obtained by modifying the distance between two rigid $ZrCp_2$ fragments. The geometry of the fragments was adapted from the experimental determination carried out for $[(C_5H_4Me)_2ZrI]_2$,[3] and the conformation of the dimer was assumed to maintain a perfect D_{2h} symmetry while avoiding as much as possible close contacts between hydrogens belonging to different Cp rings. The Zr–I bond lengths were kept constant at their experimental value of 2.916 Å[3]. Extended Hückel parameters for Zr were taken from ref 7. Ab initio SCF/CI calculations were carried out on two complexes of $(Zr)_2^{6+}$: the first one with a "short" metal–metal bond, namely, $Zr_2Cl_6(PH_3)_4$ (2) taken as a model for $Zr_2Cl_6(PEt_3)_4$ (d_{Zr-Zr} = 3.169 Å[4]); the other one with a "long" Zr–Zr bond. We selected for this calculation $[Cp_2Zr[\mu\text{-}P(CH_3)_2]]_2$ (d_{Zr-Zr} = 3.653 Å),[1] and we modeled it as $[Cp_2Zr(\mu\text{-}PH_2)]_2$ (3). Complexes 2 and 3 were assumed to have D_{2h} symmetry and experimental bond lengths and angles (Figure 1).

We selected for zirconium a (15,10,8) basis set obtained by adding a p-type orbital of exponent 0.12 to the standard set optimized by Veillard and Dedieu.[8] The contraction is [6,4,4] corresponding to a single-ζ description for the inner shells and the 5p shell, double-ζ for 5s, and triple-ζ for 4d. The most diffuse exponent for the valence d shell is 0.133 882, and the maximum of the associated density distribution is located 1.77 Å from the nucleus. The basis set taken for phosphorus in the phosphine ligands is the (11,7) set optimized by Huzinaga[9] and contracted into [4,3]. For the bridging phosphido groups, the same basis set was incremented with one s-type and one p-type diffuse function, both of exponent 0.04. A similar (12,8) basis set, contracted into [5,4], was used for all chlorine atoms. It was obtained by adding one s-type and one p-type function, both of exponent 0.06, to the standard Huzinaga basis set. Basis sets of respective sizes (9,5) and (4) were used for carbon and hydrogen and contracted to split valence. The SCF calculations were then carried out by using the ASTERIX system of programs,[10] whereas the configuration interaction expansions were performed by using Siegbahn's contracted CI program.[11]

(1) Chiang, M. Y.; Gambarotta, S.; van Bolhuis, S. *Organometallics* **1988**, *7*, 1864–1865.
(2) Wielstra, Y.; Gambarotta, S.; Meetsma, A.; de Boer, J. L. *Organometallics* **1989**, *8*, 250–251.
(3) Wielstra, Y.; Gambarotta, S.; Meetsma, A.; Spek, A. L. *Organometallics* **1989**, *8*, 2948–2952.
(4) Cotton, F. A.; Diebold, M. P.; Kibala, P. A. *Inorg. Chem.* **1988**, *27*, 799–804.
(5) Gambarotta, S.; Chiang, M. Y. *Organometallics* **1987**, *6*, 897–899.
(6) (a) Hoffmann, R. *J. Chem. Phys.* **1963**, *39*, 1397–1412. (b) Hoffmann, R.; Lipscomb, W. N. *Ibid.* **1962**, *36*, 2179–2189, 3489–3493; **1962**, *37*, 2872–2883.
(7) Tatsumi, K.; Nakamura, A.; Hofmann, P.; Stauffert, P.; Hoffmann, R. *J. Am. Chem. Soc.* **1985**, *107*, 4440–4451.
(8) Veillard, A.; Dedieu, A. *Theor. Chim. Acta* **1984**, *65*, 215–218.
(9) Huzinaga, S. Technical Report; University of Alberta: Edmonton, 1971.
(10) (a) Ernenwein, R.; Rohmer, M.-M.; Bénard, M. *Comput. Phys. Commun.* **1990**, *58*, 305–328. (b) Rohmer, M.-M.; Demuynek, J.; Bénard, M.; Wiest, R.; Bachmann, C.; Henriet, C.; Ernenwein, R. *Ibid.* **1990**, *60*, 127–144. (c) Wiest, R.; Demuynek, J.; Bénard, M.; Rohmer, M.-M.; Ernenwein, R. *Ibid.*, in press.
(11) Siegbahn, P. E. M. *Int. J. Quantum Chem.* **1983**, *23*, 1869–1889. The CI program was interfaced with ASTERIX by C. Daniel, M.-M. Rohmer, and M. Speri.

0276-7333/91/2310-0157$02.50/0 © 1991 American Chemical Society

Table I. Configuration Interaction Expansions Carried Out on the Lowest Singlet and Triplet States of $Zr_2Cl_6(PH_3)_4$ (2) (d_{Zr-Zr} = 3.169 Å) and $Cp_2Zr_2(PH_2)_2$ (3) (d_{Zr-Zr} = 3.653 Å)

	complex 2				complex 3			
	expansion 1		expansion 2		expansion 1		expansion 2	
	^1A_g	$^3B_{1u}$	^1A_g	$^3B_{1u}$	^1A_g	$^3B_{1u}$	^1A_g	$^3B_{1u}$
no. of correlated electrons	30	30	2	2	18	18	6	6
no. of MOs[a]	31	31	50[b]	50[b]	34[b]	34[b]	68[b]	68[b]
reference configurations	2	1	2	1	2	1	3	2
σ natural orbital population	1.765	1.000	1.700	0.992	1.758	0.999	1.721	0.997
σ^* natural orbital population	0.230	0.998	0.290	0.982	0.217	0.953	0.271	0.994
total enegy,[c] hartrees	−0.9846	−0.9354	−0.9663	−0.9289	−0.1656	−0.1247	−0.1608	−0.1220
correlation energy, hartrees	0.0701	0.0230	0.0516	0.0165	0.0620	0.0429	0.0572	0.0402
S–T separation, cm^{-1}			8200				8500	

[a] Doubly occupied, active, and virtual orbitals selected for the CI expansion. [b] Restricted to irreducible representations A_g and B_{1u}. [c] Shifted by 11 185 hartrees for complex 2 and by 8515 hartrees for complex 3.

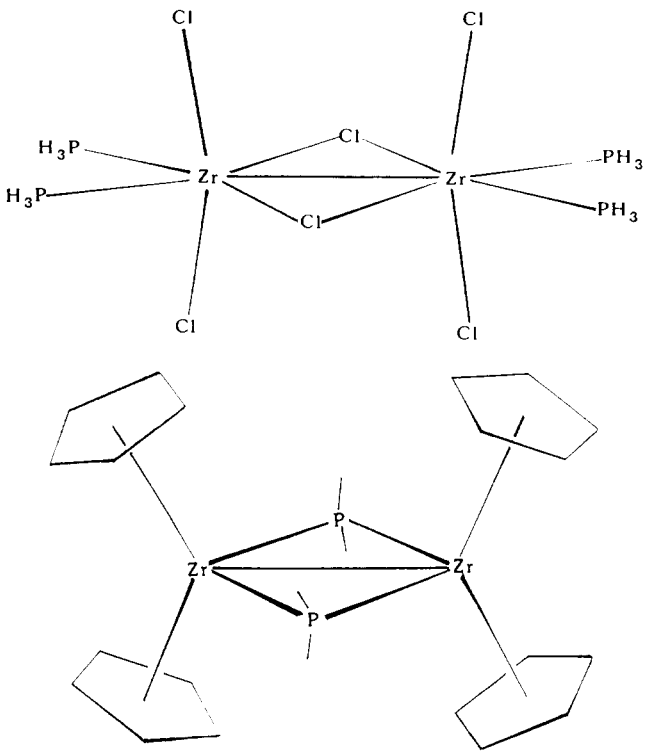

Figure 1. Plot of the model molecules used for the ab initio calculations: (a) $Zr_2Cl_6(PH_3)_4$ (2), (b) $[(C_5H_5)_2Zr(\mu\text{-}PH_2)]_2$ (3). The metallacycles are assumed to be in the *yz* plane, with *z* collinear to the Zr–Zr axis.

Configuration Interaction

One of the goals of the present ab initio calculations was to obtain a reliable estimate of the singlet–triplet energy separation for complexes 2 and 3, which requires the correlation effects to be accounted for. In order to maintain a balanced description of both the metal–metal and the metal–ligand interactions in the correlated wave function, a two-step procedure was used:

Step 1. Starting from the molecular orbitals optimized at the SCF level for the lowest singlet state (σ^2 configuration), a CI expansion was carried out with respect to the σ^2 and the σ^{*2} reference configurations over a limited set of frontier orbitals, both occupied and virtual (expansion 1). The natural orbitals associated with expansion 1 and their occupation numbers were derived and used as orbital basis for the CI expansions of the next step. An expansion involving the same orbital space was also carried out with respect to the unique triplet reference $\sigma^1\sigma^{*1}$ in order to characterize the most important configurations.

Step 2. Assuming that the major correlation effects involve those of the strongly occupied natural orbitals whose occupation has decreased significantly, the orbitals with occupation numbers higher than 1.99 e are kept frozen in the next expansions. The remaining electrons are then correlated with respect to the complete virtual space through a multireference CI expansion, taking as references all configurations with coefficients higher than 0.1 in expansion 1, singlet or triplet. It was then shown on complex 2 that the restriction of the virtual space to the sets of virtual orbitals belonging to representations A_g and B_{1u} (i.e., respectively containing the σ and σ^* orbitals) did not decrease the correlation energy by more than 2.7×10^{-4} hartrees. This restricted virtual space was therefore adopted for molecule 3. These CI expansions, carried out for the ground-state singlet and for the lowest triplet states, are referred to as expansion 2. The characteristics and results of expansions 1 and 2 are displayed in Table I. Although the energy associated with expansion 2 is slightly higher than that computed for the same state with expansion 1 because of the reduced number of correlated electrons, the final calculation provides a much more reliable and stable estimate of the singlet–triplet energy separation.

Qualitative Analysis of Orbital Interactions

The metal–metal and the metal–iodine interactions occurring in the Zr_2I_2 plane of $[Cp_2ZrI]_2$ (*yz* plane) are represented in Figure 2, together with the variation of the correspnding energy levels (obtained from extended Hückel calculations) as a function of the distance between the $Zr(Cp)_2$ fragments. Four low-lying orbitals, of respective symmetry B_{3g}, A_g, B_{1u}, and B_{2u}, appear in that order at metal–metal distances larger than 3.75 Å. These orbitals represent the four combinations of the p_y and p_z orbitals of iodine with either the doubly occupied metal–metal σ-bonding orbital (thus giving rise to one four-electron destabilizing interaction) or with the unoccupied metal–metal combinations of appropriate symmetry (generating three stabilizing interactions). The sum of the energies of these four orbitals is approximately constant for distances between 3.05 and 3.85 Å. Beyond this distance, the energy of the b_{2u} orbital steeply increases because of the combination of two factors originating in the deformation of the Zr_2I_2 rhombus: (i) the reduction of the I–I distance enhances the destabilizing character of the out-of-phase combination of the p_y iodine orbitals, and (ii) the bonding character of the metal–ligand interaction tends to vanish with the decrease of the I–Zr–I angle. For metal–metal distances below 3.85 Å, the stability of the complex therefore seems to be conditioned by the HOMO, a Zr–Zr σ-bonding orbital with A_g symmetry, slightly destabilized (~0.4 eV) due to its antibonding interaction with the proper combination of iodine p_y orbitals (Figure 2).

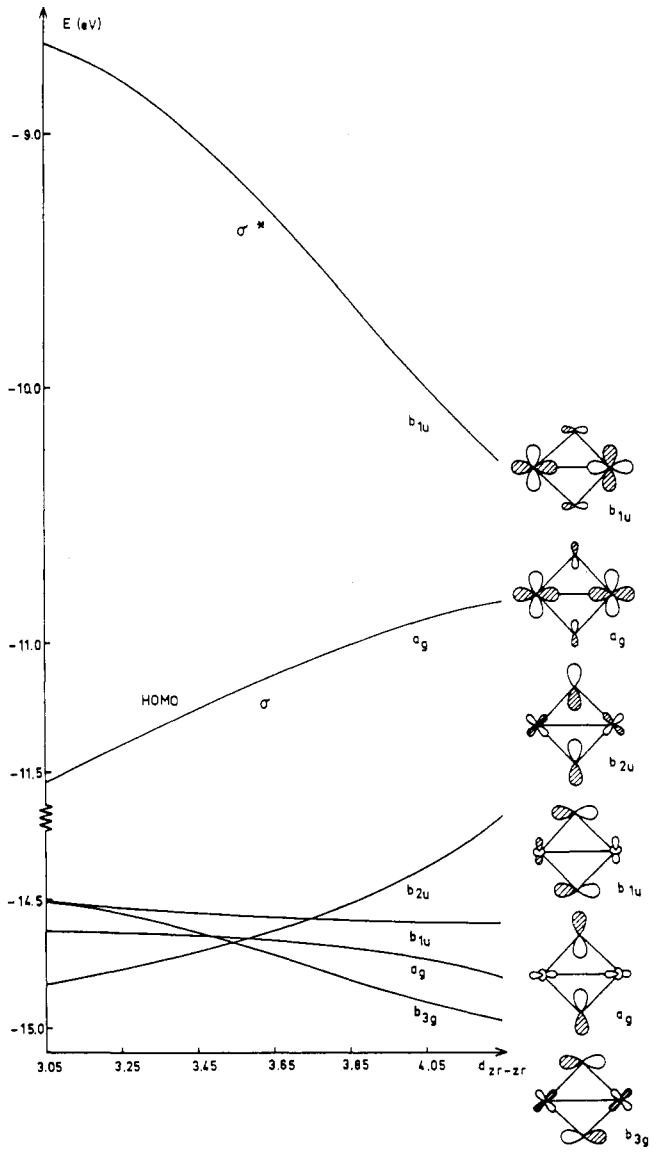

Figure 2. Energies of the Zr–Zr σ and σ^* orbitals and of the p_y and p_z orbital combinations of the bridging ligands in $Cp_2Zr_2(\mu\text{-}I)_2$ as a function of the metal–metal distance (from extended Hückel calculations).

It must be noted that the energy of the HOMO is steadily increasing with the Zr–Zr distance between 3.05 and 4.25 Å.[12] This is our first hint that a significant through-space Zr–Zr bonding character could persist at very large distances. Although this statement may seem provocative, it is consistent with the evolution of the σ–σ^* orbital energy gap (Figure 2). Starting from 3 eV at d_{Zr-Zr} = 3 Å, the gap remains as high as 1.8 eV at 3.65 Å and still reaches a nonnegligible value of 0.5 eV at 4.25 Å. It is clear, however, that such a conclusion cannot be claimed if based upon the sole criterion of extended Hückel (EH) calculations. Woolley[13] has shown that the current EH parametrization used for metal atoms tends to overestimate the d–d overlap as a compromise to incorporate effects that do not appear in the one-electron stabilization energy, such as electron correlation and core-valence orthogonality. The existence of a through-space interaction at large distances therefore requires confirmation from ab initio calculations (see the next section).

Going back to the diagram of Figure 2, it is clear that the orbital interactions displayed there do favor a *short* metal–metal bond. In spite of that, the potential energy curve associated with these EH calculations has its minimum at d_{Zr-Zr} = 4.05 Å. The origin of such a large equilibrium distance obviously resides in a serious steric hindrance involving the Cp rings that face each other in a direction collinear to the metal–metal axis. Assuming the Cp–Zr–Cp angle to retain the experimental value of 130.13° found for $[(C_5H_4Me)_2ZrI]_2$,[3] severe repulsive H···H contacts do appear even at large metal–metal distances. If the Cp rings are assumed to be eclipsed, four contacts with $d_{H\cdots H}$ = 2.0 Å develop between the $ZrCp_2$ moieties at d_{Zr-Zr} = 3.65 Å, whereas the shortest H···H distance inside a given fragment is 2.1 Å. A first estimate of the energetical effect of H···H contacts was obtained through ab initio SCF calculations on two coplanar benzene molecules approaching each other. This simulation indicates that the energy cost of two H···H interactions at 2.0 Å is close to 2 kcal mol^{-1}, to be doubled since we want to mimic *two* pairs of interacting cycles. In order to refine this model, we investigated the interactions of two C_5H_5 cycles, reproducing the eclipsed conformation and the geometrical parameters used in the calculation of $[(C_5H_5)_2Zr(\mu\text{-}PH_2)]_2$ for two C_5H_5 ligands in the cis position. Each C_5H_5 molecule was assumed to be neutral, with an open-shell electronic configuration, in order to avoid an irrelevant electrostatic repulsion. The SCF energy was −383.926 76 hartrees, to be compared with −383.931 71 hartrees for two isolated Cp rings. The destabilization is therefore 3.1 kcal mol^{-1} for *one* pair of interacting cycles, that is, higher than 6 kcal mol^{-1} for the complete system, not including the contacts between adjacent ligands (i.e., coordinated to the same metal atom).

Let us suppose now that the metal–metal distance in $[Cp_2Zr(PH_2)]_2$ is reduced by 0.6 Å, from 3.65 to 3.05 Å. It can be postulated as a first approximation that the distance between the Cp centroids is decreased by the same amount. A SCF calculation has been carried out to test the effect of H···H repulsions assuming this hypothesis. The energy of Cp···Cp jumps to −383.891 32 hartrees, corresponding to a destabilization of 25.3 kcal mol^{-1} with two cycles and 50.6 kcal mol^{-1} with four cycles. If the complete ligand system composed of four Cp cycles is considered, however, one can expect that value to be overestimated since the strong repulsive contacts could certainly be amended, accounting for the facile variation of the Cp–Zr–Cp angle between 115° and 135°.[1-3,5] This flexibility is nevertheless limited by the increasing effect of H···H contacts between the *adjacent* Cp rings. The geometrical optimization of the Cp_4 model of our dizirconium molecule was carried out at the SCF level as a function of the Cp–Zr–Cp angle, still assuming a distance of 3.05 Å between the dummy Zr atoms. The optimized energy for Cp_4 was −767.8024 hartrees, corresponding to an overall destabilization of 38 kcal mol^{-1} with respect to four isolated Cp cycles. The order of magnitude of the destabilization induced by the H···H contacts therefore appears sufficient to prevent a decrease of the metal–metal bond length. It is of interest to notice that the fulvalene dicyclopentadienyl derivative $(C_{10}H_8)(CpZrI)_2$, for which the hindrance is less drastic, displays a much shorter Zr–Zr distance than the equivalent $[(C_5H_4Me)_2ZrI]_2$ complex (3.472 Å compared to 3.649 Å).[3] Similarly, the fulvalene derivative $(C_{10}H_8)(CpZrCl)_2$ could be characterized with

(12) This energy variation cannot be attributed to a modification of the metal–iodine antibonding interaction. Similar calculations carried out on the $ZrCp_2$ dimer (without bridging ligands) show that the Zr–Zr σ-bonding orbital is just shifted down in energy by a quasi-constant amount of 0.4 eV over the whole range of considered distances.

(13) (a) Woolley, R. G. *Nouv. J. Chim.* **1981**, *5*, 219–225, 227–232. (b) Woolley, R. G. *Inorg. Chem.* **1985**, *24*, 3519–3525.

Table II. Net Charges and Metal Orbital Populations in $Zr_2Cl_6(PH_3)_4$ (2), $Zr_2Cp_4(PH_2)_2$ (3), and the Associated Molecular Fragments $[ZrCl_2(PH_3)_2]^+$ (4) and $[ZrCp_2]^+$ (5) (from ab Initio Calculations)[a]

	2	4	3	5
5s	0.25	0.34	0.32	0.25
5p	0.53	0.41	0.40	0.37
$4d_{2z^2-x^2-y^2}$[b]	0.98	0.91	0.80	0.63
$4d_{x^2-y^2}$	0.67	0.62	0.78	0.77
$4d_{xy}$	0.23	0.23	0.43	0.55
$4d_{xz}$	0.27	0.25	0.39	0.51
$4d_{yz}$	0.43	0.28	0.44	0.13
net metal charge	+0.63	+0.96	+0.43	+0.79
diffuse character,[c] %	44.0	30.0	47.2	36.6

[a] Cl level for the dimers, SCF level for the monomers. [b] z collinear to the Zr–Zr direction (see Figure 1). [c] Contribution of the most diffuse Gaussian function to the population of the $4d_{z^2}$ orbital.

a short Zr–Zr distance of 3.233 Å,[5] whereas the equivalent chlorine-bridged complex of the Cp_2Zr dimer remains elusive.[3] We suggest that the observed variation of the thermal stability in the $(Cp_2ZrX)_2$ complexes according to the order I > Br > Cl[3] results from the decrease of the Zr–X equilibrium distance according to the same order. Assuming that the optimal Zr–X–Zr angle remains approximately constant, the congestion of the molecule will preclude the characterization of any stable product with Br or a fortiori with Cl, unless the constraints are eased by replacing two Cp rings by a fulvalene ligand.

Ab Initio SCF/CI Calculations: Results and Discussion

The results of the CI calculations carried out on $Zr_2Cl_6(PH_3)_4$ (2) (d_{Zr-Zr} = 3.169 Å) and on $Zr_2Cp_4(PH_2)_2$ (3) (d_{Zr-Zr} = 3.653 Å) are displayed in Table I. In spite of the different metal–metal distances, the results obtained for both molecules are strikingly similar. The natural orbital analysis of the singlet ground state obtained from CI expansion 2 yields orbital populations $\sigma^{1.70}\sigma^{*0.29}$ for 2 and $\sigma^{1.72}\sigma^{*0.27}$ for 3. Such a distribution of the σ and σ^* orbital populations is characteristic of a relatively strong metal–metal bond. An antiferromagnetic coupling, either through-bond or through-space, would imply a more balanced distribution. The high population of the σ-bonding orbital in the covalent singlet ground state is consistent with the large singlet–triplet energy splitting computed for both molecules, 8200 and 8500 cm^{-1} for 2 and 3, respectively. Surprisingly enough, the S–T splitting, together with the σ population, tends to *increase* with the Zr–Zr distance. An analysis of the HOMO in 2 and 3 shows that the zirconium dimer responds to an increase of the metal–metal bond length by an expansion in space of the σ-bonding orbital. In the short-bonded complex 2, the distribution of the $4d_{z^2}$ population over the two most diffuse basis functions is rather balanced, 0.41 and 0.47 e (0.40 and 0.49 e in the SCF wave function). The relative weight of the most diffuse function is 44.0%, accounting for the contribution of the innermost valence Gaussian-type orbital (GTO). In the long-bonded complex 3, the distribution becomes 0.30 and 0.43 e (SCF: 0.28 and 0.48 e) and the most diffuse component clearly outweighs the intermediate one. The weight of the most diffuse Gaussian function increases to 47.2% (Table II). As a consequence, the density generated by the σ bond along the metal–metal axis decreases very slowly with the Zr–Zr distance.

The persistence of a significant metal–metal bonding interaction at distances larger than 3.5 Å therefore has its origin in a high polarizability of the 4d σ metal orbital. Such a flexibility appears unexpected from a metal atom displaying a formal charge of +3, since a high positive charge should result in a rather contracted and hardly polarizable valence shell. In fact, the real net charge of the metal atoms, as obtained from the Mulliken population analysis of the Cl wave function, is no more than slightly positive, +0.63 e for 2, and +0.43 e only for 3 (Table II), which helps us understand the flexibility of the σ-bonding orbital. The correlation between the polarizability of the σ orbital and the metal atomic net charge can be pushed further by reporting the Mulliken analysis of the SCF wave function computed for the monomeric fragments $[ZrCl_2(PH_3)_2]^+$ (4) and $[ZrCp_2]^+$ (5). Although Zr formally remains +3 in those fragments, the positive net charge on the metal is obviously higher in the cationic fragments than in the neutral dimer, namely, +0.96 e for 4 and +0.79 e for 5. In close correlation with these values, the d_{z^2} orbital appears rather contracted in 4 (weight of the most diffuse component: 30.0%), somewhat less in 5 (36.6%), but consistently less expanded in space than in the respective dimers (Table II, Figure 4).

Coming back to the dimers, a part of the extra charge with respect to an isolated Zr^{+3} atom comes from covalent interactions with the coordination sphere, as illustrated by the populations of the 5s and 5p shells: $5s^{0.25}5p^{0.53}$ for 2, $5s^{0.32}5p^{0.40}$ for 3.[14] Globally considered, the population of shell 5 is only slighly modified compared to that obtained in the cationic fragments (Table II). The rest of the electron density comes from the bonding interactions of the unoccupied d orbitals with the surrounding ligands. The populations of the metal orbitals that are not directly involved in the major interactions with either the bridging ligands or the other metal ($d_{x^2-y^2}$, d_{xz}, d_{xy}) are not drastically modified with respect to their values in the cationic fragments. Some charge transfer is, however, observed, especially in 3 around the metal atoms from the outside to the inside of the metallacycle. More specifically, a significant increase of the d_{yz} population is obtained in the dimers, as a result of the stabilizing metal–bridging ligand interactions. One should also notice a consistent increase of the $4d_{2z^2-x^2-y^2}$ population when going from the fragment to the dimer. This population changes from 0.91 e in fragment 4 to 0.98 e in the associated dimer 2 and, still more remarkable, from 0.63 e in fragment 5 to 0.80 e in the long-bonded dimer 3. At the same time, the corresponding increase in the population of the $d_{z^2-y^2}$ orbital is either moderate or unsignificant (Table II). This surge in the population of the $d_{2z^2-x^2-y^2}$ metal orbitals, together with their expansion in space, confirms that the formation of a metal–metal σ bond is one of the driving forces leading to the stabilization of both the short-bonded and the long-bonded dimers.

The electron density generated by the σ-bonding natural orbitals of dimers 2 and 3 has been represented in Figure 3, a and b, respectively. A standard population of two electrons has been assigned to both orbitals, in order to make the plots comparable. In both complexes, the HOMO is broadly $d_{z^2-y^2}$, with the largest coefficient on z^2 in 2 but on y^2 in 3. In complexes bridged by halogen atoms, the lobe on y^2 reduces the metal–ligand antibonding

(14) (a) Low, J. J.; Goddard, W. A., III. *J. Am. Chem. Soc.* **1984**, *106*, 6928–6937. (b) Low, J. J.; Goddard, W. A., III. *Ibid.* **1986**, *108*, 6115–6128. (c) Low, J. J.; Goddard, W. A., III. *Organometallics* **1986**, *5*, 609–622. (d) Wisner, J. M.; Bartczak, T. J.; Ibers, J. A.; Low, J. J.; Goddard, W. A., III. *J. Am. Chem. Soc.* **1986**, *108*, 347–348. (e) Brandemark, U. B.; Blomberg, M. R. A.; Pettersson, L. G. M.; Siegbahn, P. E. M. *J. Phys. Chem.* **1984**, *88*, 4617–4621. (f) Bäckvall, J. E.; Björkmann, E. E.; Pettersson, L.; Siegbahn, P. *J. Am. Chem. Soc.* **1984**, *106*, 4369–4373; **1985**, *107*, 7265–7267. (g) Bäckvall, J. E.; Björkmann, E. E.; Pettersson, L.; Siegbahn, P.; Strich, A. *Ibid* **1985**, *107*, 7408–7412. (h) Blomberg, M. R. A.; Siegbahn, P. E. M.; Bäckvall, J. E. *Ibid.* **1987**, *109*, 4450–4456.

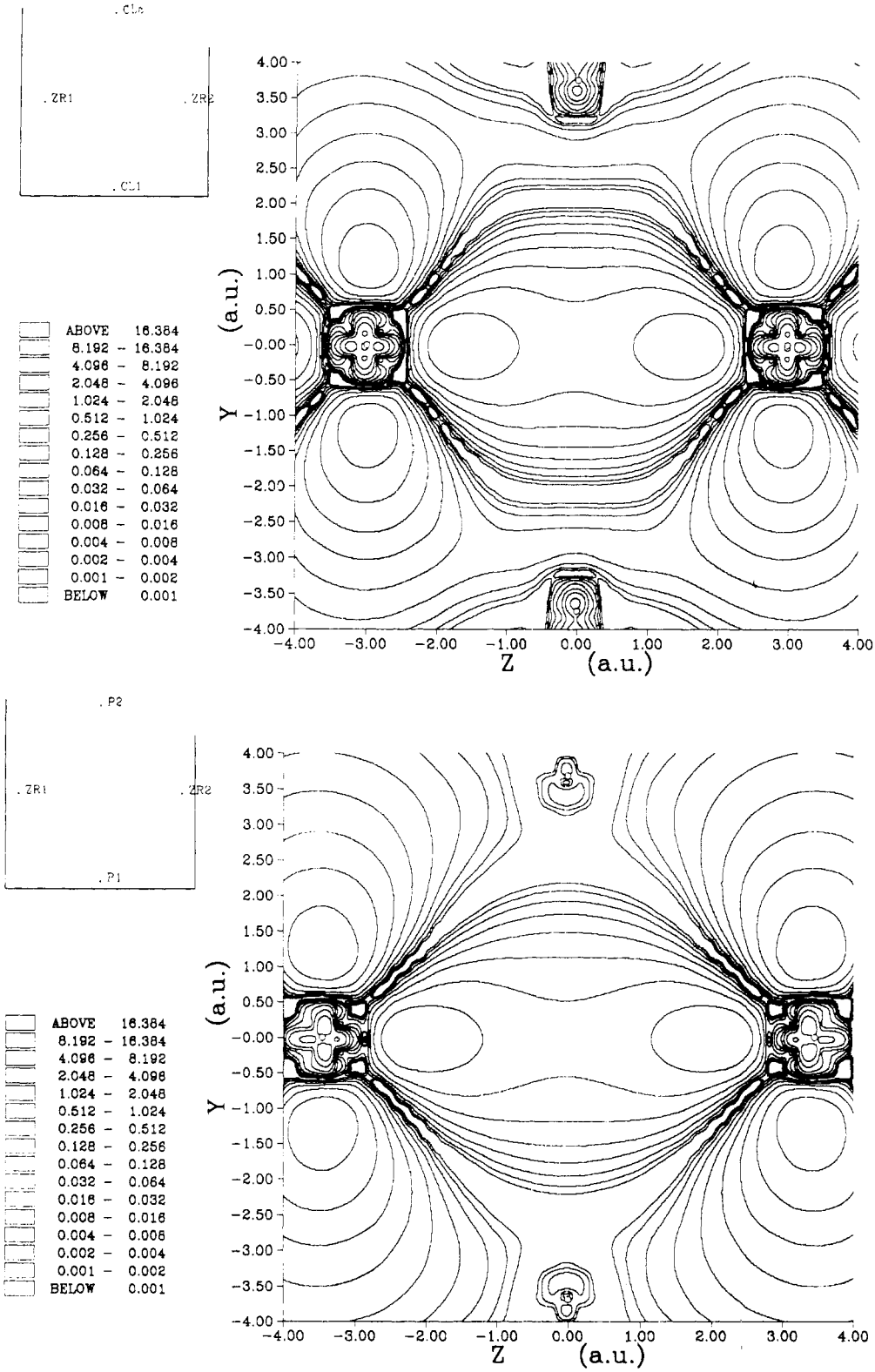

Figure 3. Plot of the electron densities associated with the metal–metal σ natural orbitals in $Zr_2Cl_6(PH_3)_4$ (a) and $[Cp_2Zr(\mu\text{-}PH_2)]_2$ (b). The represented plane contains the Zr atoms and the bridging ligands. The outermost contour corresponds to a density of 0.001 e Å^{-3}. Thereafter, contours differ by a factor of 2.

character in the $(ZrX)_2$ metallacycle and introduces some through-bond metal–metal coupling, as can be seen from Figure 3a. No such interaction exists, however, in the HOMO of the phosphido-bridged complex (Figure 3b), but the $d_{z^2-y^2}$ orbital is stabilized by an interaction with the π^* orbital of the Cp cycles. In this latter molecule, the density at the center of the Zr–Zr bond has decreased with respect to the short-bonded complex, but not so drastically as could have been expected: it still reaches at 3.65 Å the appreciable value of ~0.1 e Å^{-3}.

Deformation density maps were computed as the difference between the total density of the molecular CI wave function and the sum of densities computed for the molecular fragments $[ZrCl_2(PH_3)_2]^+ + [ZrCl_2(PH_3)_2]^+ + [Cl_2]^{2-}$ for **2** and $[ZrCp_2]^+ + [ZrCp_2]^+ + [(PH_2)_2]^{2-}$ for **3**. At variance from deformation densities obtained from a superposition of spherical atoms, fragment deformation densities are known to provide information relatively easy

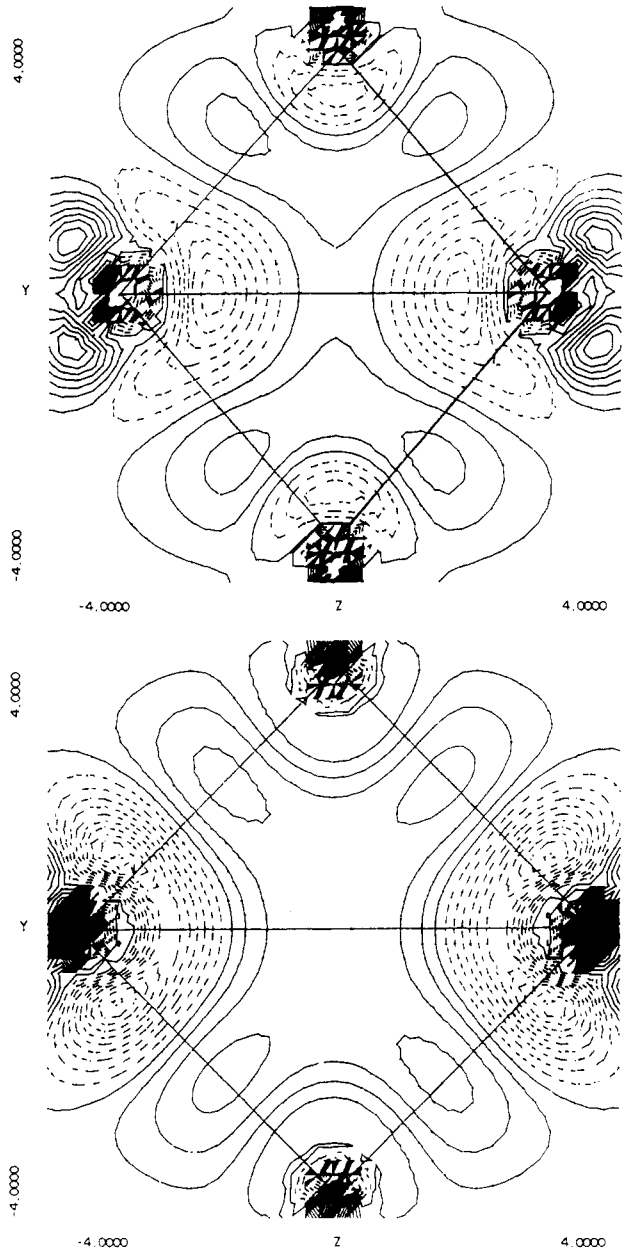

Figure 4. Plot of the electron deformation densities with respect to a superposition of molecular fragments: (a) $Zr_2Cl_6(PH_3)_4$; (b) $[Cp_2Zr(\mu\text{-}PH_2)]_2$. The represented plane contains the Zr atoms and the bridging ligands. Solid lines correspond to zero and positive density, dotted lines to negative density. Contour interval 0.025 e Å^{-3}.

to interpret in terms of bonding,[15] since they eliminate most of the contribution due to atomic hybridization.[16] The map obtained for **2** (Figure 4a) is characterized by a double minimum of density along the metal–metal axis at ~0.7 Å from the metal atoms. Beyond these minima is found a shallow, X-shaped accumulation of density extending over a very large region of space from the center of the metal–metal axis to the vicinity of the bridging atoms. This accumulation has a double maximum along the *y* axis, located 0.8 Å above and below the Zr–Zr line and corresponding to a value of 0.04 e Å^{-3}. The density at the center of the metal–metal bond is 0.02 e Å^{-3}. The accumulation then extends toward the *yz* direction, culminating into four maxima (0.05 e Å^{-3}), approximately located on the Zr–Cl lines. This map is characteristic of an expansion in space of the $d_{z^2-y^2}$ molecular orbital with respect to the fragment orbital, as described above from the analysis of the Mulliken populations. The density minima correspond to the depopulation of the intermediate GTO describing the 4d orbital to the benefit of the most diffuse function. This explains the extension in space and the shallowness of the accumulation region. The maxima along the Zr–Cl bonds illustrate the increase of the d_{yz} orbital population in the dimer (0.43 e, compared to 0.28 e in the fragments). In that sense, these maxima are a direct consequence of the Zr–Cl bonding interactions.

The density map obtained for **3** (Figure 4b) is qualitatively similar (depopulation around the zirconium atoms, large X-shaped accumulation extending from the center of the metal–metal bond to the Zr–P bonds), but the electron reorganization appears more important in the present case, leading to deeper minima on the one hand, to higher and more extended accumulations on the other hand. The region surrounding the center of symmetry corresponds to a large plateau of deformation density (0.070 e Å^{-3}). This is at variance from the distribution obtained for **2**, in which the center of the metallacycle was a saddle point (note that these topological differences arise from density variations less than 0.025 e Å^{-3} and do not clearly appear from the contours of Figure 4). This plateau results from the expansion of the d orbitals and also from the electron reorganization affecting the $ZrCp_2$ fragments. Table II shows that this reorganization globally increases the population of the $4d_{2z^2-x^2-y^2}$ metal orbital by 0.17 e, thus accounting for the large central accumulation. Beside, the population transfer into the d_{yz} orbital due to the metal–PH_2 interactions reaches 0.31 e (Table II), yielding, as for **2**, four peaks centered on the Zr bridge line. These peaks are higher than for **2** (0.08 e Å^{-3}), illustrating the rise of the transfer of density into the d_{yz} orbital (Table II).

A comparison of the two maps of Figure 4, without referring to other sources of information, such as the Mulliken population analyses of Table II, may appear surprising. As a matter of fact, those maps display a density accumulation higher and more extended at the center of the *long* Zr–Zr bond (complex **3**) than along the *short* metal–metal bond in **2**. One should not consider, however, the height of the density peak as a direct measure of the bond strength. The deformation density peaks arise from a *relative* modification of the shape and population of the $d_{2z^2-x^2-y^2}$ metal orbitals with respect to the characteristics of the same orbital in the isolated fragments. In fact, the *absolute* population of the $d_{2z^2-x^2-y^2}$ metal orbitals has been reduced from 0.98 e in the short-bonded dimer to 0.80 e in the long-bonded one (Table II). Assuming a similar delocalization of the σ bond for both molecules (justified by the natural orbital analysis of the CI expansions), this can be interpreted in the sense of a weak but real decrease of the σ bond strength in **3**. The comparison of the density plots for the σ orbitals in both dimers (Figure 3) provides arguments in the same direction. The interpretation we propose for the fragment deformation density of Figure 4b is as follows: in spite of the long Zr–Zr distance, the dimer still can afford an important reorganization of the electron population in the $ZrCp_2$ fragments, resulting in an increase of the density around the center of the metal–metal axis, i.e., in the formation of a metal–metal σ bond. The other driving force toward the stabilization of

(15) Hall, M. B. In *Electron Distributions and the Chemical Bond*; Coppens, P., Hall, M. B., Eds.; Plenum Press: New York, 1982; pp 205–220.

(16) (a) Kunze, K. L.; Hall, M. B. *J. Am. Chem. Soc.* **1986**, *108*, 5122–5129; **1987**, *109*, 7617–7623. (b) Schwarz, W. H. E.: Valtazanos, P.; Ruedenberg, K. *Theor. Chim. Acta* **1985**, *68*, 471–506. (c) Schwarz, W. H. E.; Mensching, L.; Valtazanos, P.; von Niessen, W. *Int. J. Quantum Chem.* **1986**, *29*, 909–914.

the dimer consists of metal–PH_2 interactions mainly involving the $4d_{yz}$ orbitals of zirconium (Figure 2).

The results obtained in the present work are not completely unambiguous, however. We stress here the unusual persistence at very long distances of a well-characterized σ-bonding orbital with significant overlap population. This through-space model of bonding cannot be considered as the sole driving force ensuring the stability of the molecule. Shaik et al. have discussed the intricacy of through-space and through-bond interactions in bridged M_2L_{10} complexes.[17] The five occupied orbitals displayed in Figure 2, including the metal–metal σ MO, have contributions on both the metal and the bridging atoms and participate to the through-bond interaction, as noticed by Shaik et al.[17] Other through-bond interactions, not considered in the present work, could rely upon the acceptor potentialities of the bridging ligands. These potentialities are extremely reduced for chlorine ions, but they could be enhanced for the iodine or phosphido ligands in relation with the presence of an empty low-lying d shell. The calculations on $[Cp_2Zr(\mu\text{-}PH_2)]_2$ discussed in the present work did not include d orbitals on the P atoms. Preliminary SCF calculations carried out on the same molecule with more extended basis sets for the Zr and the P atoms indicate that d orbitals on phosphorus (Gaussian exponents 0.9 and 0.3) could have some influence, more as polarization functions than as acceptor valence orbitals, however.[18] We suggest that the respective contributions of the through-space and through-bond interactions could be studied in more detail by comparing, at the same metal–metal distance, the characters and properties of the $[Cp_2Zr(\mu\text{-}PH_2)]_2$ molecule to those of a hypothetic nonbridged system with same through-space metal–metal interactions, such as $[Cp_2Zr]_2^{2+}$. This comparison will be carried out in a forthcoming study.

(17) Shaik, S.; Hoffmann, R.; Fisel, C. R.; Summerville, R. H. *J. Am. Chem. Soc.* **1980**, *102*, 4555–4572.

(18) The most important d populations on phosphorus are on d_{xy} (0.09 e) and on d_{z^2} (0.07 e). Other d orbital populations are less than 0.015 e. Most of that population comes from an electronic reorganization internal to the phosphido groups rather than from a back-donation effect. The net charge of each phosphido group is −0.25 e with the basis set including d functions, compared to −0.20 e with the standard basis set.

Conclusion

Extended Hückel calculations carried out on dinuclear complexes of zirconium(III) at distances between 3.05 and 4.25 Å suggest the presence of a substantial amount of through-space metal–metal interaction at distances larger than 3.5 Å. This indication is confirmed by a thorough analysis of the ab initio SCF/CI wave function obtained for $Zr_2Cl_6(PH_3)_4$ (d_{Zr-Zr} = 3.169 Å) and $Zr_2Cp_4(PH_2)_2$ (d_{Zr-Zr} = 3.653 Å). The population of the σ-bonding natural orbital for both complexes (respectively 1.700 and 1.721 e) and the singlet–triplet energy separations (8200 and 8500 cm^{-1}) are computed to be approximately similar for both molecules. The insensitivity of the Zr–Zr diamagnetic coupling to the bond length is attributed to an expansion in space of the d_{z^2} atomic orbitals, which accompanies the elongation of the Zr–Zr bond, leading to a very slow decrease of the σ overlap population.[19]

Acknowledgment. The quantum chemical calculations have been carried out with the CRAY-2 computer of the Centre de Calcul Vectoriel de la Recherche (Palaiseau, France), through a grant of computer time from the Conseil Scientifique du CCVR.

(19) After this work had been sent to the Editor, we became aware of local spin density calculations carried out by R. L. De Kock and leading to similar conclusions.[20]

(20) De Kock, R. L. Unpublished, private communication.